Cool-Climate or Warm-Spike Lateritic Bauxites at High Latitudes?

Gregory J. Retallack

Department of Geological Sciences, University of Oregon, Eugene, Oregon 97403, U.S.A.
(e-mail: gregr@uoregon.edu)

ABSTRACT

Laterites and bauxites and their associated Ultisols and Oxisols are widespread in warm-wet climates today, and their spread to high latitudes has been attributed to episodes of past global warming. Bauxitic paleosols from the Early Eocene Monaro Volcanics of southeastern Australia have been claimed as exceptions formed in a cool-wet climate. Reexamination and chemical analysis of a sequence of intrabasaltic paleosols in the Bega no. 7 core of radiometrically dated Monaro Volcanics now show highly variable paleotemperature and precipitation. The core includes 53 successive paleosols, mostly nonbauxitic, but bauxitic paleosols reveal local spikes in warmth and precipitation coincident with early Eocene (55-, 52-, 51-, and 48-Ma) global spikes of warmth, precipitation, and high atmospheric CO_2. These bauxitic paleosols thus formed in warm-wet, not cool-dry, climates, and their poleward spread coincided with global greenhouse spikes.

Introduction

Bauxites and laterites and their soils (Oxisols and Ultisols) are common in warm-wet climates today, and their appearance at high paleolatitudes in the geological past has been attributed to global warming events (Parrish 1998). The paleotemperature significance of laterites and bauxites was challenged by Taylor et al. (1992), who documented lateritic bauxites with 40% gibbsite, 35.2 wt% Al_2O_3, and 19.0 wt% Fe_2O_3 from the Early Eocene Monaro Volcanics of southeastern Australia (fig. 1), which was then at a paleolatitude of 57° ± 4°S (Idnurm 1985). Taylor et al. (1992) argued that factors other than temperature control laterite and bauxite formation, such as aluminous parent material, efficient leaching, high precipitation (Paton and Williams 1972), long duration of formation (Taylor et al. 1992), high atmospheric CO_2 (Bird et al. 1990), near-surface alteration of outcrops (Hunt et al. 1977), or continuous long-term alteration of surface outcrops (Bourman 1993).

This study reexamines intrabasaltic bauxitic and other paleosols of the Monaro Volcanics in deep drill core, unaffected by surface or continuous alteration. Parent material, drainage, precipitation, temperature, CO_2, and duration of soil formation, as confounding factors in anomalous Monaro bauxites of Taylor et al. (1992), are here reevaluated to determine the paleoclimatic significance (if any) of lateritic bauxites.

Manuscript received May 6, 2008; accepted August 11, 2008.

Materials Examined

Stratigraphic sections of paleosols were measured and sampled from Bridle Creek (S36.231667°, E148.968333°, elevation 955 m), Wambrook Hill (S36.21117°, E148.926667°, 1100 m), Hudsons Peak (S36.44167°, E149.165833°, 1230 m), Rock Flat (S36.392067°, E149.2155°, 900 m), and the Bega no. 7 core near Lake Myalla (S36.40497°, E149.11759°, 1115 m). Field observations of four paleosols and core observations of 53 paleosols fell into seven distinct pedotypes (tables 1, 2), named using the local Naringo (Narrugu) language (Mathews 1908). Hand specimens of all moderately to strongly developed paleosols were analyzed by x-ray fluorescence for major-element composition by ALS-Chemex of Vancouver, British Columbia (table 3). Basalt analyses were not undertaken as part of this research, but 137 analyses compiled by Roach (1999) are averaged in table 3.

Geological Setting of Monaro Volcanics

The Monaro Volcanics is about 630 km^3 of largely alkali olivine basalts from an intraplate volcanic field of some 65 separate fissures, maars, and small cinder cones (fig. 1; Pratt et al. 1993; Roach 1994,

[The Journal of Geology, 2008, volume 116, p. 558–570] © 2008 by The University of Chicago.
 0022-1376/2008/11606-0002$15.00 DOI: 10.1086/592387

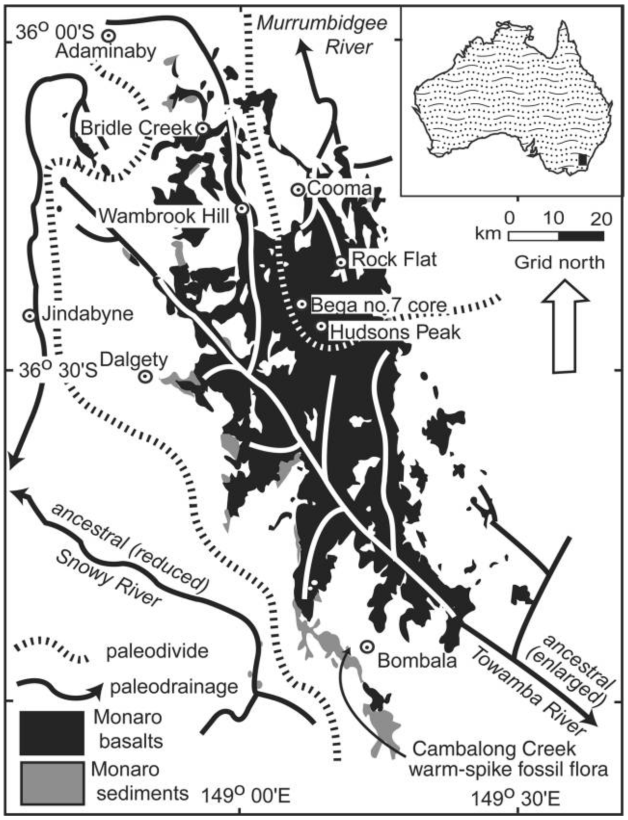

Figure 1. Distribution of Monaro Volcanics and Eocene paleodrainage (after Roach 1996), with location of the Bega no. 7 core and other field localities.

1996). Lavas filled preexisting hilly terrain with relief of at least 500 m (Taylor et al. 1990) and elevation of as much as 1000 m (Holdgate et al. 2008). The lavas have K-Ar ages of late Paleocene–Eocene (56–34 Ma; Wellman and McDougall 1974; Roach 1996). These ages have been corrected for outdated analytical constants, where necessary, using the tables of Dalrymple (1979). The dated Bondo flow in the Bega no. 7 core can be combined with five other K-Ar dates of flows of known stratigraphic level at nearby Hudsons Peak and Rock Flat to provide interpolated geological ages for every level within the core (fig. 2). The Bondo flow is a distinctive marker bed in outcrop, enabling correlations along the Cooma-Myalla and the Cooma-Bega roads within a 12-km radius of the Bega no. 7 drill hole (Roach 1999). The flows were from fissure eruptions or shield volcanoes of low relief and wide extent (Roach 1996). The standard error on the age model regression of figure 2 is ±1.5 Ma, comparable with errors on individual age determinations (table 1). These are all K-Ar dates, and new dating using $^{39}Ar/^{40}Ar$ methods is desirable, but such redating in other sequences showed improved precision but little difference in age model (Retallack et al. 2004). Numerous other radiometric dates from the Monaro Volcanics are tabulated by Roach (1999) and Sharp (2004) but were not used here because they were distant and difficult to correlate with the core.

Burial Alteration of Paleosols

Alteration of paleosols after burial must be considered before proceeding with paleoenvironmental interpretations that might be compromised by such alteration. The smectite-rich paleosols of Taylor et al. (1990) were considered hydrothermal alteration zones by Sharp (1994), but Brown et al. (1994) countered that alteration is gradational down from sharp basal flow contacts, not symmetrical around intensely clayey zones. My own observations confirm this, as well as root traces, clay skins, and peds ("spontaneous cracking" of Sharp 1994), indicative of dilational alteration at the surface rather than penetrative alteration under burial or hydrothermal pressure. Furthermore, potash content does not increase with alumina enrichment (fig. 3), as would be expected with burial or hydrothermal illitization (Nesbitt and Young 1989; Rainbird et al. 1991).

Table 1. K-Ar Age Dates Used for Age Model

Location	Sample type	Stratigraphic level (m)	Original date (Ma)	Corrected date (Ma)	Error (Ma)
Hudson Peak flow, elevation 1230 m	Whole rock	−115	40.2	42.2	1.6
Hudson Peak flow, elevation 1190 m	Whole rock	−75	45.1	46.3	.8
Bondo flow, Bega no. 7 core	Whole rock	66	48.9	48.9	.3
Near basal flow, elevation 905 m, Rock Flat	Whole rock	191	52.7	54.1	.9
Basal flow, elevation 900 m, Rock Flat	Whole rock	196	53.1	54.5	1.2
Basal flow, elevation 900 m, Rock Flat	Whole rock	196	54.4	55.8	1.0

Note. Dated rocks in and around the Bega no. 7 core are listed from Wellman and McDougall (1974) and Roach (1996); corrections of older dates to new constants follow Dalrymple (1979). Negative stratigraphic levels are in a hill above the top of the core, drilled down from 1115-m elevation.

Table 2. Recognition and Identification of Paleosols

Pedotype	Meaning	Diagnosis	U.S. taxonomy	FAO classification
Birrin	Ashes	Gray surface (A) over clay-enriched brown (7.5YR) subsurface (Bt) and then mottled weathered (Bg) and fresh basalt	Hapludalf	Plinthic Luvisol
Dhaguk	Black	Carbonaceous surface (A) over gray clay (Bg) and mottled basalt (Bg)	Aquept	Plinthic Gleysol
Gurubang	Stone	Thin brown (10YR–7.5YR) oxidized surface (A) over leached and then fresh basalt	Orthent	Lithosol
Kabbatch	Pipe clay	Grayish-brown surface (A) over thick, red (5YR), clay-enriched (Bt) and then deeper mottled (Bg) and fresh basalt	Hapludult	Plinthic Acrisol
Kubiangi	Small	Thin gray-green surface (A) over red mottled clay on fresh basalt	Aquent	Plinthic Gleysol
Ngaiur	Red ochre	Gray surface clay (A) over very thick red (2.5YR) subsurface (Bo) and then mottled basalt (Bg) and fresh basalt at depth	Udox	Dystric Nitosol
Ngulla	Flesh	Grayish-brown surface (A) over brown (7.5YR) weathered basalt (Bw) and then deeper mottled (Bg) and fresh basalt	Ochrept	Gleyic Cambisol

Note. Aboriginal names are from Mathew (1908). FAO, Food and Agriculture Organization.

Sharp (1994) suspected intrastratal hydrothermal alteration during burial, but acidic waters and gases near mofettes (volcanogenic CO_2 vents) can also deforest and acidify soils before burial by overlying flows (Stephens and Hering 2002). No comparable vent facies were noted in the core or in any local silicification. Deforestation is not evident from the paleosols, which have abundant fossil root traces in the core. Furthermore, the titania/alumina ratios of all 41 paleosol samples are very similar (0.13 ± 0.04, mean ± SD, from data of table 4) and indistinguishable from those in 137 analyses of parent basalts (0.14 ± 0.03, from data of Roach 1999). Conserved stoichiometry of weather-resistant elements is characteristic of weathering, not acidification, as also found in a comparable basalt-hosted paleosol study (Sheldon 2006).

As in baking effects of other intrabasaltic paleosols quantified using vitrinite reflectance and ceramicization (Sheldon 2003), Monaro intrabasaltic paleosols show no more than 5 cm of surficial baking, recognizable as indurated surfaces, some-

Table 3. Interpretation of Paleosols

Pedotype	Climate	Vegetation	Topographic setting	Parent material	Time for formation (k.yr.)
Birrin	Humid (1035 ± 182 mm MAP), cool temperate (16.3° ± 4.4°C MAT), seasonal	Cool temperate rainforest	Well-drained flows	Vesicular basalt	10–100
Dhaguk	Humid (1080 ± 182 mm MAP), cool temperate (15.6° ± 4.4°C MAT), seasonal	Seasonally dry swamp	Poorly drained depression	Basaltic sand	.1–1.0
Gurubang	Not diagnostic for climate	Early successional woodland	Well-drained flows	Vesicular basalt	.1–1.0
Kabbatch	Humid (1352 ± 182 mm MAP), warm temperate (17.1° ± 4.4°C MAT), seasonal	Warm temperate rainforest	Well-drained flows	Vesicular basalt	10–100
Kubiangi	Humid (1005 ± 182 mm MAP), cool temperate (15.2° ± 4.4°C MAT), seasonal	Seasonally dry swamp	Poorly drained depression	Vesicular basalt	.1–1.0
Ngaiur	Humid (1372 ± 182 mm MAP), warm temperate (17.1° ± 4.4°C MAT), seasonal	Warm temperate rainforest	Well-drained flows	Vesicular basalt	100–500
Ngulla	Humid (853 ± 182 mm MAP), cool temperate (14.9 ± 4.4°C MAT), seasonal	Cool temperate rainforest	Well-drained flows	Vesicular basalt	5–10

Note. MAP, mean annual precipitation; MAT, mean annual temperature.

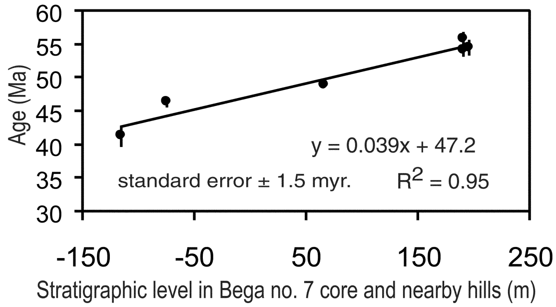

Figure 2. Age model of Monaro Volcanics (data from Wellman and McDougall 1974; Roach 1996).

times discolored. The greatest discoloration was seen in the surface (A) horizon of a Ngaiur paleosol in the Bridle Creek outcrop, which was brownish yellow (10YR6/8) but was yellowish red (5YR5/8) in an indurated surface 5 cm thick. The chilled lower margin of flows was presumably an excellent insulator from thermal alteration of parts of paleosols sampled for this study.

Bega No. 7 Paleosol Sequence

The Bega no. 7 core recovered 95% of 198.2 m of Eocene Monaro Volcanics, over 8.5 m of Paleocene sandstones and coals, and 9.0 m of Paleozoic basement metamorphosed sandstone and schist (Brown et al. 1992). The flows include vesicular olivine tholeiites and transitional basalts near the base, with alkali olivine basalts near the middle and the top (fig. 4). Flow surfaces are variably weathered to 53 successive smectite-rich and kaolinite-rich paleosols. Each paleosol is capped abruptly by a chilled margin of the overlying flow.

The 53 paleosols in the Bega no. 7 core can be grouped into seven pedotypes (fig. 5) and classified in U.S. soil taxonomy (Soil Survey Staff 2000), using a combination of profile observations (table 2) and geochemical data (table 4). Some profiles are thin and very weakly developed, such as Entisols (Kubiangi, Gurubang), whereas others have deeper profiles but without clay accumulation, which would qualify as argillic (Ngulla, Dhaguk). These paleosols are distinguished by red-brown (Gurubang, Ngulla) or gray-green (Kubiangi, Dhaguk) color. Among the argillic paleosols, molar ratios of alumina/bases less than 2 distinguish Alfisols (such as Birrin) from Ultisols and Oxisols (Retallack 2001*b*). Oxisols (Ngaiur) have gibbsite and a thickness much greater than that of Ultisols (Kabbatch). Strongly developed paleosols (Ngaiur and Kabbatch) are rare in the core and regionally in outcrop, notably at Bridle Creek (Taylor et al. 1992).

Paleosol Record of Paleoenvironments

Features and classification of paleosols can be evidence for past environmental controls on soil formation (table 5) and its extreme manifestation as bauxitization at a few stratigraphic levels in the Monaro Volcanics. The diversity of pedotypes and the rarity of bauxites are indicative of highly changeable conditions of soil formation through time.

Paleoclimate. How cool and wet it was during the formation of bauxitic and other paleosols can be assessed from the chemical composition of B horizons of the moderately developed paleosols. For example, the chemical index of alteration without potash ($C = 100\ \mathrm{mAl_2O_3}/(\mathrm{mAl_2O_3} + \mathrm{mCaO} + \mathrm{mNa_2O})$, in mol) increases with mean annual precipitation (R, in mm) in modern soils (eq. [1], with $R^2 = 0.72$; SE = ±182 mm from Sheldon et al. 2002). The training set of modern soils for this compilation was found from climates with precipitation raging from 200 to 1600 mm, and results from Monaro paleosols do not exceed these limits (fig. 6*A*):

$$R = 221e^{0.0197C}. \tag{1}$$

Paleotemperature of paleosols can be derived from alkali content ($S = (\mathrm{mK_2O} + \mathrm{mNa_2O})/\mathrm{mAl_2O_3}$, in

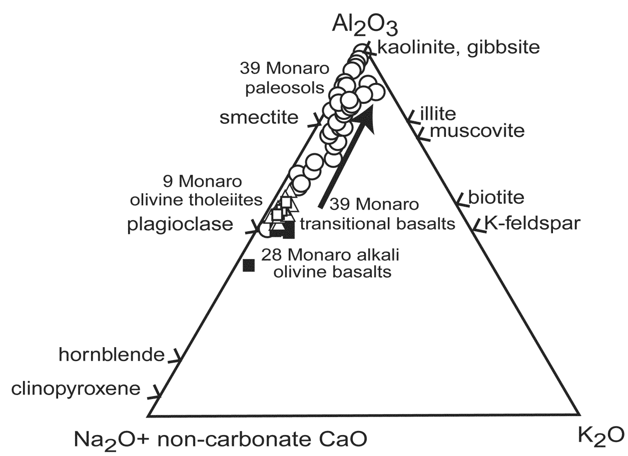

Figure 3. Weathering trends in the chemical data, showing no divergence toward potassic compositions expected if paleosols are altered by burial diagenesis and very low alumina content of parent materials. Paleosol analyses are given in table 3 (two with secondary calcite excluded), and basalt analyses are from Roach (1999).

Table 4. Whole-Rock Chemical Analysis of Paleosol B Horizons and Basalt Parent Rocks

Level (m)	SiO_2	Al_2O_3	Fe_2O_3	CaO	MgO	Na_2O	K_2O	Cr_2O_3	TiO_2	MnO	P_2O5	SrO	BaO	LOI	Total
3.3	37.04	14.5	11.47	2.65	6.67	.28	.13	.02	2.54	.58	.96	.04	.04	23	99.92
7.9	33.05	20.1	19	1.01	2.82	.01	.08	.05	2.93	.08	.09	.01	.03	20.6	99.88
12.5	38.88	13.09	10.62	4.6	7.76	.57	.87	.04	1.54	.17	2.09	.03	.03	19.6	99.89
15.4	41.02	14.08	12.85	1.87	6.19	1.01	1.3	.04	2	.13	.4	.04	.05	18.95	99.92
16.2	39.5	11.53	14	2.96	7.26	.84	1.35	.05	2.02	.15	1.29	.02	.04	18.6	99.61
22.6	42.25	13.48	11.68	3.13	7.21	.74	1.2	.03	1.26	.15	.76	.21	.06	17.75	99.91
30.5	20.15	28.15	16.67	.7	2.59	.01	.03	.05	5.4	.25	.42	<.01	.04	25.1	99.55
35.1	23	25.75	18.48	.58	1.47	.03	.07	.14	4.91	.2	.35	<.01	.04	24.5	99.53
44.3	33.19	22	15.01	.82	2.34	.14	.58	.06	3.23	.1	.11	.01	.04	22.1	99.73
52.6	38.75	13.78	11.94	2.08	10.59	.75	1.09	.03	1.81	.15	.35	.02	.04	18.55	99.94
53.5	37.18	17.68	15.62	1.79	5.17	.38	.93	.05	2.72	.16	.37	.01	.06	17.7	99.8
64.5	36.08	15.54	14.28	2.08	8.67	.41	.88	.04	2.21	.19	.26	.02	.04	19	99.69
66.1	39.46	18.15	12.11	2.13	3.45	.28	1.15	.04	2.63	.07	.18	.02	.05	20.3	100
68.4	39.15	18.02	13.18	1.84	2.89	.15	.17	.05	2.75	.03	.03	.01	.02	21.7	100
78.8	38.32	15.14	13.85	3.5	7.28	.68	1.27	.03	1.91	.12	.32	.02	.04	17.2	99.69
93.2	17.08	34.25	12.7	.44	1.09	.15	.05	.17	10.78	.12	.37	<.01	.04	22.5	99.7
94.8	27.59	23.74	19.74	2.3	2.54	.17	.1	.04	4.02	.12	.84	.08	.07	18.45	99.79
100.1	29.05	22.28	27.46	.64	.92	.22	.09	.04	3	.07	.17	.01	.06	15.8	99.81
102.4	28.95	21.27	20.03	2.87	3.06	.16	.1	.06	2.44	.34	.21	.02	.04	20.2	99.74
114.7	21.16	10.57	8.64	16.35	8.68	.37	.58	.02	.89	.81	.21	.04	.02	31.4	99.73
117.4	25.7	18.18	30.47	.79	2.05	.17	.13	.05	2.39	.07	.47	.02	.04	19.4	99.92
118.9	19.13	30.57	24.22	.34	1.04	.11	.05	.1	3.89	.09	.43	.01	.04	19.9	99.92
127.0	27.87	20.73	15.51	5.96	4.07	.21	.08	.03	3.11	.24	.12	.01	.04	21.9	99.88
127.6	27.26	27.08	20.49	1.02	1.15	.18	.05	.03	4.1	.15	.35	.02	.05	17.35	99.29
134.4	36.18	21.5	14.99	1.17	1.73	.26	.21	.03	2.58	.11	.13	<.01	.03	21	99.94
136.3	36.88	21.02	14.77	1.81	2.15	.4	.48	.03	2.54	.14	.18	.02	.04	19.4	99.86
138.4	35.06	16.08	12.13	7.72	2.56	.5	.85	.03	1.95	.48	.46	.03	.03	21.7	99.57
149.7	38.7	15.4	10.89	6.94	5.5	1.69	.96	.03	1.74	.22	.45	.06	.06	17.05	99.7
150.0	23.45	8.47	6.13	27.61	4.49	.21	.24	.03	.74	.76	.61	.03	.01	26.5	99.29
155.3	30.66	10.63	7.84	9.7	6.82	.62	.64	.04	1.06	.27	.28	.06	.04	31.2	99.84
157.4	35.33	13.27	11.81	6.37	6.17	.33	.4	.04	1.46	.18	.33	.02	.02	24.1	99.86
164.1	41.17	17.33	12.03	2.92	5.13	1.25	.98	.05	2.08	.08	.52	.04	.05	15.95	99.56
184.4	38.22	16.03	12.71	1.89	9.53	.6	.53	.04	1.86	.11	.15	.01	.03	18.2	99.93
186.3	38.5	15.45	14.41	1.57	8.19	.82	.81	.04	1.81	.08	.36	.02	.03	17.55	99.62
187.3	41.11	16.49	11.56	1.75	7.07	.99	.98	.05	1.88	.06	.38	.01	.04	17.05	99.42
191.5	43.24	15.83	7.59	2.39	5.36	.77	.92	.04	1.71	.05	.35	.02	.03	21.3	99.6
192.8	40.98	14.74	10.74	3.37	5.48	.61	.81	.05	1.7	.13	.32	.03	.03	20.8	99.79
197.4	41.17	13.65	8.75	5.87	5.85	.17	1.08	.02	1.07	.29	.05	.02	.02	21.8	99.8
197.9	50.85	15.93	5.28	1.03	4.16	.21	1.22	.03	1.39	.04	.04	.03	.04	19.65	99.89
200.3	43.45	17.58	5.48	1.83	4.64	.4	.77	.06	1.97	.03	.75	.08	.03	22.7	99.78
202.2	55.7	17.66	3.08	.66	2.61	.24	1.23	.04	1.51	.01	.03	.01	.03	16.85	99.68
202.7	59.7	16.52	2.56	.5	1.85	.16	1.77	.03	1.13	.01	.04	.01	.04	15.4	99.71
Error	2.705	.825	.395	.22	.18	.11	.13		.06	.025	.035			.35	
Alk.ol.	46.29	14.72	11.53	9.88	8.39	2.90	1.48	.03	2.05	.16	.63	.10	.05	2.58	100.02
Error	1.27	1.79	1.59	1.82	3.01	.79	.81	.03	.56	.02	.29	.04	.04	1.75	1.52
Basan.	43.70	14.11	11.56	9.78	10.04	3.47	1.66	.04	2.34	.17	1.01	.15	.07	2.41	99.82
Error	2.00	2.09	1.06	1.72	3.58	1.47	.94	.03	.70	.03	.64	.14	.05	1.79	1.17
Thol.	47.05	14.39	12.00	8.64	9.62	2.56	.88	.04	1.55	.15	.37	.07	.03	3.72	100.29
Error	1.67	.91	.83	1.29	1.26	.61	.23	.03	.21	.03	.10	.09	.03	3.06	2.22
Trans.	46.65	14.64	11.50	9.00	9.10	2.69	1.12	.03	1.80	.15	.49	.09	.04	2.93	99.74
Error	1.89	1.09	3.16	1.62	2.41	.61	.54	.02	.37	.03	.20	.09	.04	2.05	2.12

Note. Analyses are from samples of the Bega no. 7 core stored in Geoscience Australia, Canberra, by x-ray fluorescence from ALS-Chemex of Vancouver, British Columbia, using CANMET standard SDMS2. Errors for paleosols are 2 SD of 10 replicate analyses of the standard. Analyses and errors of 28 alkali olivine basalts, 58 basanites, 9 olivine tholeiites, and 39 transitional basalts are averaged from Roach (1999). LOI, loss on ignition.

mol), which decreases in modern soils with mean annual temperature (T, in °C; using eq. [2], with $R^2 = 0.37$; SE = ±4.4°C from Sheldon et al. 2002). The standard error of these estimates is disappointingly large, but the 2°–20°C temperature range of this climofunction is not exceeded by results from Monaro paleosols (fig. 6*B*):

$$T = -18.5S + 17.3. \qquad (2)$$

Confirmation of these warm paleotemperatures comes from prior isotopic analyses. Kaolinite from the Bridle Creek exposure of a Ngaiur paleosol, dated by K-Ar as 47.7 ± 0.5 Ma (Sharp 2004), was analyzed for oxygen and hydrogen isotopic composition by Bird and Chivas (1989; $\delta^{18}O_{SMOW}$ + 18.8‰, δD_{SMOW} − 74‰, where SMOW is standard mean ocean water). This oxygen isotopic value is comparable with that of recent tropical soil clays of Cameroon ($\delta^{18}O_{SMOW}$ + 17‰ to +19.5‰) but less than that for those of Hawaii ($\delta^{18}O_{SMOW}$ + 21‰ to +25‰; Bird et al. 1990). The Ngaiur kaolinite falls on a cross plot of hydrogen and oxygen isotopic compositions within the domain of modern soil kaolinites (so not hydrothermal, diagenetic, or nonanalog paleoclimate) and is compatible with a formation temperature of 22° ± 3°C (Tabor and Montañez

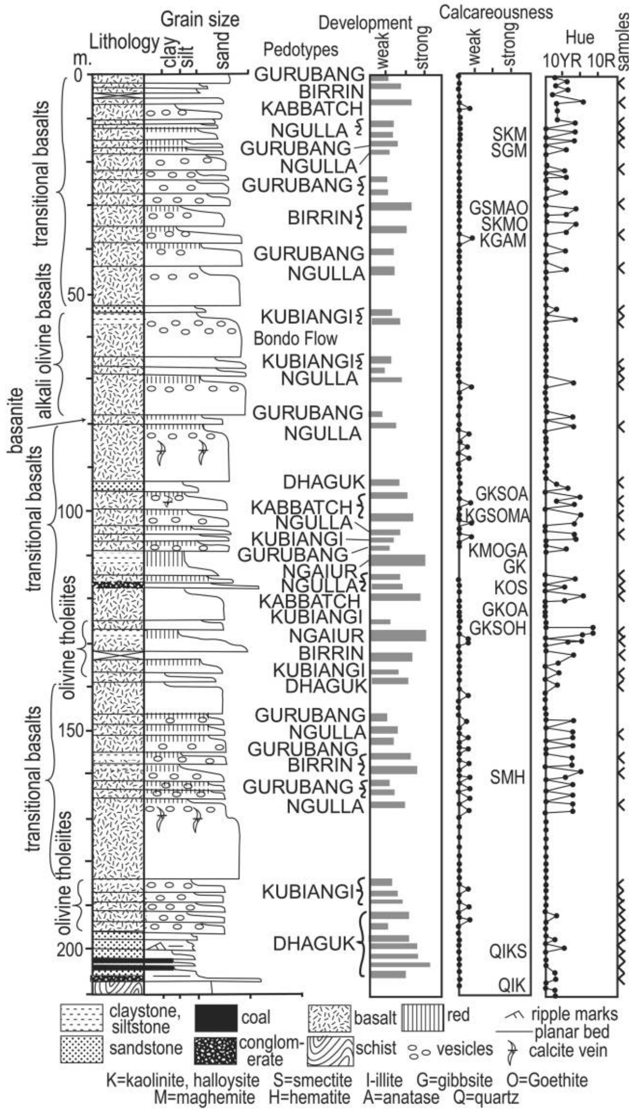

Figure 4. Paleosols in the Bega no. 7 core. Paleosol locations are indicated by bars in development column, and samples chemically analyzed in this article are in the right-hand margin. Mineral composition of selected samples is from Brown et al. (1992). Paleosol development bars and scale of calcareousness from field acid application are from Retallack (2001*b*), with hue after a Munsell chart. Basalt types are from Roach (1996).

2005), comparable with alkali maximum paleotemperatures from paleosols (fig. 6*B*).

Another way of analyzing the paleoclimate of Monaro Volcanic intrabasaltic paleosols is to calculate climatic energy ($E =$ kJ m^{-2} yr^{-1}) used by the individual paleosols, which combines effects of both precipitation and temperature (effective energy and mass transfer [EEMT] of Rasmussen and Tabor 2007). This can be calculated from data on modern basalt soils, using the chemical index of alteration (C, defined as for eqq. [1], [3]; $R^2 = 0.93$, SE $= \pm 3259$ kJ m^{-2} yr^{-1}). With a training set range of 13,000–35,000 kJ m^{-2} yr^{-1} from the southern Cascade Range of California, values calculated for Monaro paleosols are an extrapolation toward levels found in warmer and wetter climates:

$$E = 542.16 \times C - 17,191. \qquad (3)$$

The paleosols show an estimated precipitation range of 1139 mm (368–1507 mm), a paleotemperature range of 4.6°C (12.7°–17.3°C), and an energy range of 43,980 kJ m^{-2} yr^{-1} (21,145–65,125 kJ m^{-2} yr^{-1}). From the derivation of EEMT given by Rasmussen and Tabor (2007), an increase in temperature of 1°C over this range gives an energy increase of 2199 kJ m^{-2} yr^{-1}, whereas a rise in precipitation of 100 mm over this range gives a similar energy increase of 2300 kJ m^{-2} yr^{-1}. Thus, temperature within the inferred range accounts for only 23% of the energy range, whereas observed precipitation changes account for all of the inferred energy change. These proportions do not include error limits, which are large, and assume modern climate-energy relationships, which may not have applied to distant times of atmospheric CO_2 values higher than modern values (Retallack 2001*a*). Nevertheless, these calculations suggest that precipitation increases were more important than temperature increases in Monaro paleosol bauxitization.

Quantitative mean annual temperature (MAT) and mean annual precipitation (MAP) estimates from paleosols (fig. 6*A*, 6*B*) are all greater than current values in Cooma (36.23°S, 149.12°E; MAT 11.1°C, MAP 502 mm), nearest the Bega no. 7 core (fig. 1), or at current likely paleolatitudes, such as modern Macquarie Island (54.5°S, 158.94°E; MAT 5.0°C, MAP 961 mm). The Monaro Tableland during the early Eocene had a paleoclimate during warm spikes comparable with that of modern Sydney (33.90°S, 151.23°E; MAT 17.5°C, MAP 1215 mm) but was at other times more like that of Hobart (42.89°S, 144.33°E; MAT 12.1°C, MAP 617 mm; http://www.bom.gov.au/climate). Thus, the climate of the Monaro Tableland during the early Eocene was not uniformly cool and wet but mostly cool and subhumid, with spikes at 55, 53, 51, and 47 Ma of warm-humid climate, represented by bauxitic Ultisols and Oxisols in the sequence.

Such soils are unusual for such high latitudes (table 5). The current latitudinal range of kaolinitic Ultisols is 48°N (north of Chehalis, Washington, U.S.A.) to 37°S (south of Auckland, NZ). For baux-

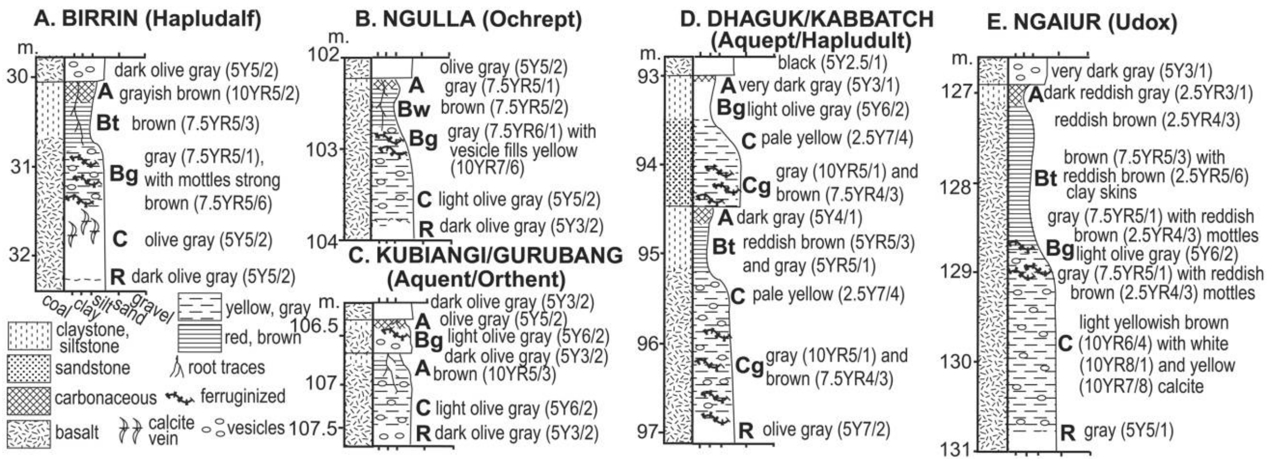

Figure 5. Paleosol pedotypes recognized in the Bega no. 7 core (Myalla Lake, elevation 1115 m). Pedotype names are from Naringo aboriginal language (Mathews 1908), and identifications are from Soil Survey Staff (2000).

itic Oxisols, the range is 23°N (north of Tepic, Mexico) to 30°S (west of Maryborough, Queensland). These ranges from soil maps (Food and Agriculture Organization 1975*a*, 1978) exclude the relict Nitosols near Cooma described here. Climatic minima for modern Ultisols are 10.8°C MAT and 1186 mm MAP and for modern Oxisols 19.5°C MAT and 1270 mm MAP (Food and Agriculture Organization 1971, 1975*a*, 1975*b*, 1978, 1979, 1981; Müller 1982; Ruffner 1985). The Monaro paleosols are thus indications of unusual periods of transient warmth at high latitudes.

Former Vegetation. Well-developed paleosols of the Bega no. 7 core have clayey root traces, sometimes filled with burial diagenetic sparry calcite and zeolite, as well as irregularities similar in shape to large roots and stumps overridden by lava flows (Birrin, Kabbatch, Ngaiur, Ngulla). Coal-bearing paleosols have large woody root traces of swamp trees (Dhaguk, Kubiangi). Root traces are less obvious in weakly developed, thin paleosols, which may have supported early successional vegetation (Gurubang).

Fossil pollen and wood in the Monaro Volcanics are like the vegetation of Tasmania today, dominated by conifers such as *Podocarpus*, *Lagarostrobus*, and *Phyllocladus* but with a diversity of angiosperms, including *Nothofagus*. Associated fossil wood was very slow growing and endured marked seasons (marked growth rings averaging 0.97 mm wide). This assemblage indicates a cool temperate rainforest with MAT 10°–14°C and MAP 1200–2400 mm (Taylor et al. 1990).

Warm spikes evident from paleosols (fig. 4) are also apparent from localities for exceptional cuticular fossil leaf preservation. The Late Paleocene (*Lygistipollenites balmei* palynozone, ca. 55 ± 0.5 Ma) Cambalong Creek flora in subbasaltic coal measures near Bombala includes *Wollemia*, Cunoniaceae, Elaeocarpaceae, *Gymnostoma*, and Lauraceae (*Beilschmedia*, *Cryptocarya*, *Endiandra*), more like living rain forest relicts of New South Wales than taxa from a Tasmanian cool temperate conifer forest. Bioclimatic analysis for this flora indicates MAT 18.5° ± 2.3°C and MAP 1980 ± 420 mm (Greenwood et al. 2003). Another comparable warm-spike flora is Hotham Heights in nearby Victoria (*Malvacipollis diversus* to *Proteacidites asperopolus* palynozones, ca. 51 ± 1 Ma, MAT 19.0° ± 2.3°C, MAP 2400 ± 450 mm; Greenwood et al. 2003). These well-preserved and diverse fossil leaf floras also fall on the climatic peaks of 55 and 51 Ma, indicated by bauxitic paleosols that also formed in a warm-humid climate more like the modern climate of Sydney than that of Hobart.

Drainage. Kubiangi and Dhaguk pedotypes are drab colored and associated with thin coal seams representing local swamps and marshes. Other Monaro paleosols with strong oxidation of iron, red colors, and deeply reaching root traces were soils of well-drained forests (Retallack 2001*b*). Nevertheless, ferruginized layers at depth in many of these paleosols (fig. 5) are similar to placic horizons (Soil Survey Staff 2000), formed in slowly draining water tables perched atop massive basalt parent material. The paleosols thus varied considerably in drainage character, and very few were freely drained, as envisaged by Paton and Williams (1972), to promote bauxitization.

Table 5. Modern Soils at Latitudinal Limits for Oxisols and Ultisols

Locality	Soil	Latitude	Longitude	Weather station	MAT (°C)	MAP (mm)	Energy (kJ m^{-2} yr^{-1})	FAO map unit
Seoul, Korea	Ultisol	37.57	126.97	Seoul	11.1	1258	36,840	Ao 84-2/3b
Sochi, Russia	Ultisol	43.58	39.72	Sochi	14.0	1356	52,763	Ao 110-2a
Porto Alegre, Brazil	Ultisol	−30.03	−51.22	Porto Alegre	19.5	1298	64,090	Ao 1-2b
Chehalis, WA, U.S.A.	Ultisol	46.72	−122.95	Centralia	10.8	1186	32,998	Ah 2-2bc
Auckland, New Zealand	Ultisol	−36.85	174.77	Auckland	15.2	1242	50,641	Ao 99-3bc
Queenstown, Australia	Ultisol	−41.10	145.50	Queenstown	14.7	2411	138,876	Ah 17-2/3c
Burgos, Philippines	Oxisol	18.37	121.63	Aparri	26.3	2118	125,285	Nd 66-2/3b
Bathurst, Gambia	Oxisol	14.73	17.5	Bathurst	25.0	1270	59,721	Nd 28-2a
Tepic, Mexico	Oxisol	23.22	−106.42	Tepic	20.0	2640	199,933	Ne 8-3b
Maryborough, Australia	Oxisol	−23.40	150.50	Pacific Heights	24.8	1305	62,428	Ne 64-2/3b
Porto Alegre, Brazil	Oxisol	−30.03	−51.22	Porto Alegre	19.5	1298	64,090	Nd 2-3c

Note. MAT, mean annual temperature; MAP, mean annual precipitation. Soil information is from the Food and Agriculture Organization ([FAO] 1971, 1975*a*, 1975*b*, 1977*a*, 1977*b*, 1978, 1979, 1981). Climatic information is from http://www.bom.gov.au, http://www.1911encyclopedia.org, and http://www.nationsencyclopedia.com and Müller (1982) and Ruffner (1985).

Parent Materials. Some Monaro paleosol profiles (five basal Dhaguk) formed on prebasaltic sediments, which may have been eroded from earlier kaolinitic and gibbsitic paleosols and so predisposed to bauxitization, as envisaged by Paton and Williams (1972). Most of the 53 paleosols, however, have relict vesicular and other igneous textures as evidence that they formed on flows of alkali olivine basalt, transitional basalt, and tholeiite. These are parent material compositions far removed from bauxite (at or near the Al_2O_3 pole in fig. 3). In addition, the fine-grained matrix of basalt impedes weathering (Retallack 2001*b*). Thus, parent material was not a significant factor in promoting bauxitization of Kabbatch and Ngaiur pedotypes.

Time between Flows. The Bega no. 7 core ranges in age from 47.2 to 55.1 Ma (fig. 2), and its rock accumulation rate of 0.004 mm yr^{-1} is identical to modern denudation rates in the region (Bishop 1985; Taylor et al. 1985; Young and McDougall 1985). A duration of 4.9 m.yr. for 50 flows of varying thickness (fig. 4) leaves an average of 98 k.yr. for soil formation between each flow.

Duration of soil formation for each paleosol (K, in k.yr.) can be estimated from the depth of solum (D, in cm), by using chronofunctions from 28–1000-k.yr. soils in humid warm temperate South Carolina (Markewich et al. 1987) and equation (4) ($R^2 = 0.80$, SE = 20 k.yr.):

$$K = 7.8133e^{0.022\times D}. \tag{4}$$

Most soil-forming durations for the Monaro Volcanics were less than the flow recurrence average, but some were longer (fig. 6*D*). Both geological and pedogenic estimates are considerably less than 1500 k.yr. for formation times of bauxites in the Monaro Volcanics estimated by Taylor et al. (1992), who also inferred 500-k.yr. durations for paleomagnetic reversals within thick paleosols. Well-dated paleomagnetic reversals are now known to be much more rapid (7.0 ± 1.0 k.yr. for 30 Quaternary reversals; Clement 2004). The Monaro bauxitic paleosols do not appear to have formed over long periods of geological time.

Comparably Spiky Records Elsewhere

There is no current record of Paleocene-Eocene atmospheric CO_2 from the Monaro Volcanics, but CO_2 and thermal maxima elsewhere were also abrupt and short-lived paleoclimatic events, like the record from the Bega no. 7 core (fig. 6).

Records of Atmospheric CO_2. The stomatal index of fossil *Ginkgo* leaves is evidence that Paleocene-Eocene warm spikes were also times of high atmospheric CO_2. Baseline Paleocene–Early Eocene values of 339 ± 52 ppmv CO_2 (mean ± SD of 26 estimates) are near modern (386 ppmv in 2007; Alley et al. 2007), but there was an earliest Eocene (55-Ma) spike of 686 ± 230 ppmv (standard error of one estimate) and an early Eocene (49-Ma) spike of 1686 ± 1066 ppmv (Retallack 2001*a*, 2008*b*). The foraminiferal boron isotopic CO_2 paleobarometer also shows baseline levels of about 400 ± 100 ppmv CO_2, with an earliest Eocene (55-Ma) spike to 950 ± 600 ppmv and an early Eocene (52-Ma) spike to 1400 ± 800 ppmv (Pearson and Palmer 2000). Late

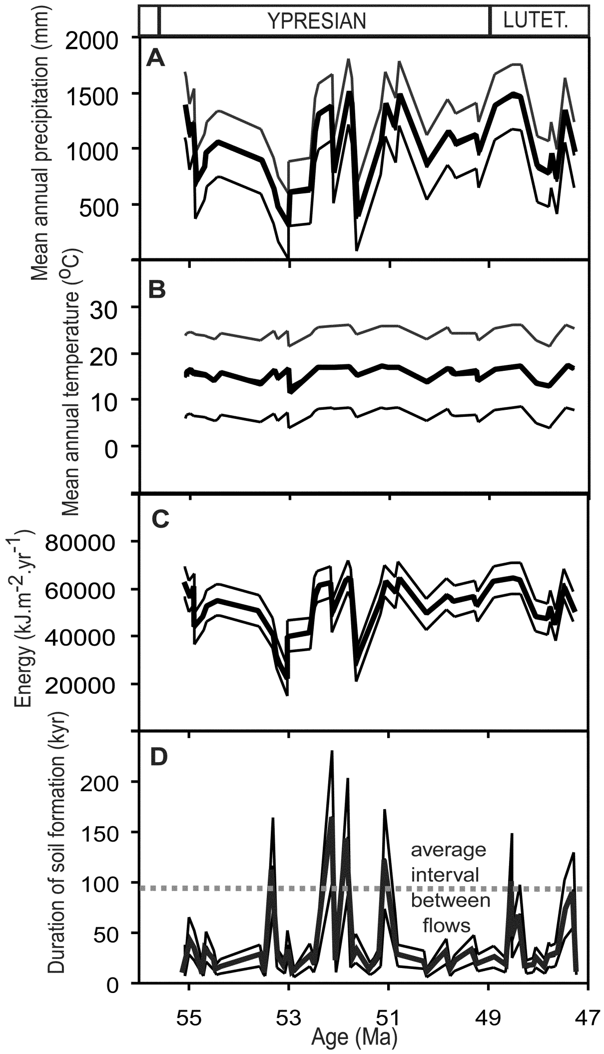

Figure 6. Time series of paleoclimatic change (*A*, *B*), energy (*C*), and duration of soil formation (*D*) from chemical analysis of Monaro Volcanic paleosols. Envelopes are all 95% confidence intervals from 2 SE of transfer functions.

Paleocene lateritic paleosols in Ireland from a high paleolatitude (55°N) have coexisting goethite and gibbsite with CO_2 mole fraction and isotopic composition compatible with those of atmospheric CO_2 levels of 2400 ± 1200 ppmv (Tabor and Yapp 2005).

High-Latitude Marine Paleoclimatic Records. Peaks of kaolinite are seen at 52 and 55 Ma in Ocean Drilling Program sites 689 and 690 in the Southern Ocean (Robert and Kennett 1992). Global compilation of foraminiferal oxygen isotopic composition (Zachos et al. 2001) is dominated by cores from the Southern Ocean and shows clear peaks of warmth at 55, 52, 51, and 49 Ma (fig. 7*B*). Shallow marine paleotemperatures estimated from oxygen isotopic composition of the bivalve *Eurhomalea* on Seymour Island, Antarctica, show temperatures of 7°–10.5°C, with spikes to 15°C at 51 and 53 Ma (Ivany et al. 2008). A 5°C warming of the Arctic Ocean from sea surface temperatures of 18°–23°C at the Paleocene thermal maximum has been estimated from the TEX_{86} marine crenarchaeotal lipid paleothermometer (Sluijs et al. 2006).

Other High-Latitude Nonmarine Records. Transient perturbation of the carbon cycle at the Paleocene-Eocene boundary is indicated by negative excursions of −2 to −6‰δ^{13}C pedogenic carbonate of aridland paleosols in Wyoming, Utah, Spain, and China (Koch et al. 1992; Bowen et al. 2005; Bowen and Bowen 2008). Evidence from oxygen isotopes and fossil soils and leaves indicates that this isotopic perturbation for some 200 k.yr. was accompanied by a transient 5°C rise in temperature in Wyoming (Wing et al. 2005; Kraus and Riggins 2007). Comparable stable isotopic shifts in paleosols of central Utah (Bowen and Bowen 2008) are coeval with a transient rise in precipita-

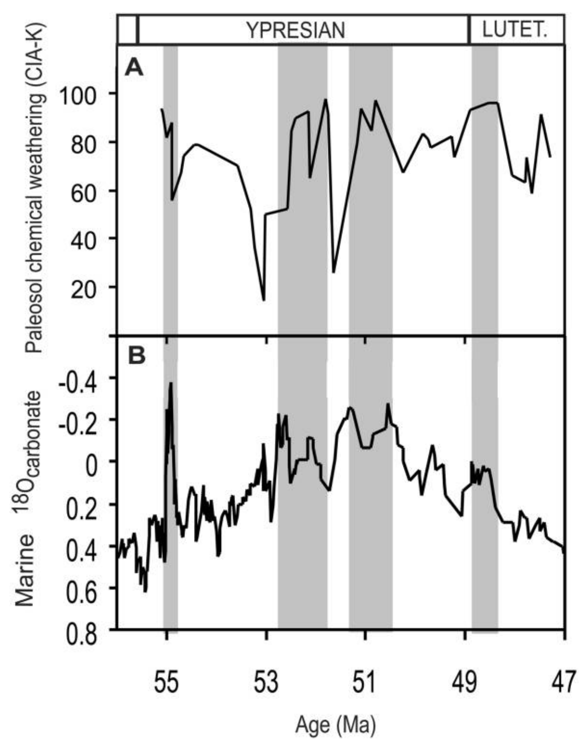

Figure 7. Chemical index of alteration (CIA-K) of Monaro paleosols (*A*) compared with oxygen isotopic composition of foraminifera in cores of the Southern Ocean (*B*; from Zachos et al. 2001). CIA-K increases with intensity of chemical weathering, and oxygen isotope values are plotted with reversed axes so that upward spikes correspond to paleotemperature increases.

tion from a background of 460 ± 147 to 779 ± 147 mm (Retallack 2005, 2008*b*).

Global warm spikes also are indicated by the spread of tropical mangroves to high latitudes (*Nypa*) in the early Eocene of Regatta Point, Tasmania (Carpenter et al. 1994; Macphail et al. 1994), and in the Early Eocene London Clay of England (Collinson 1983). Also suggestive of unusual high-latitude warmth are Paleocene and Eocene dawn redwood (*Metasequoia*) swamps of Ellesmere Island, Canadian Arctic Archipelago (Kuagai et al. 1995).

Causes of Climate Spikes. Mesozoic and Early Tertiary greenhouse paleoclimates have been considered long-lasting and stable climate modes (Parrish 1998), but detailed records of high temporal resolution are now revealing short-lived greenhouse events (Zachos et al. 2001; Bowen et al. 2005; Wing et al. 2005; Kraus and Riggins 2007) like those of the Bega no. 7 core (fig. 6). Transient paleoclimatic warming and CO_2 spikes in the geological past are of interest for anticipating future global warming and were not due to human land use or fossil fuel consumption (Alley et al. 2007). Suggested causes of anomalous warm spikes include peat production of methane with global warming (Pancost et al. 2007), comet impact (Kent et al. 2003), orbital forcing (Lourens et al. 2005), methane clathrate release (Dickens et al. 1995), and thermogenic methane from igneous intrusion of carbonaceous sediments (Svensen et al. 2004).

Conclusions

The Eocene paleoclimate of southeastern Australia was highly variable, with cool-subhumid climates interrupted by short-lived spikes of warm-humid climates (fig. 6) at times of high atmospheric CO_2 (Pearson and Palmer 2000; Retallack 2001*a*, 2008*b*). This study confirms warm-temperature dependence of bauxites (Parrish 1998) but also shows codependence on high rainfall (Paton and Williams 1972) and high CO_2 (Bird et al. 1990). All three covary during Paleocene and Early Eocene greenhouse spikes and appear to be linked in Earth's climate system (Retallack 2008*b*). Monaro paleosols were not "cool climate bauxites" formed over long periods of time (contrary to Taylor et al. 1992).

Monaro bauxitic Oxisols required MAT above 17°C, MAP above 1372 mm, and pCO_2 above 686 ppmv (fig. 8). Monaro kaolinitic Ultisols required similar temperatures and pCO_2 levels but MAP above 1161 mm. Other kinds of paleosols formed when these conditions were not met (fig. 4). Inferred paleoclimatic limits of Ultisols and Oxisols formed at elevated CO_2 can be contrasted with climatic minima of modern Ultisols and Oxisols (table 5), formed largely at pCO_2 levels of 280 ppmv (preindustrial of Alley et al. 2007). There is no significant change in temperature or precipitation minima for bauxitic Oxisols with elevated CO_2, but kaolinitic Ultisol paleosols did not form at such low temperatures and energies as did modern examples (fig. 8). There is thus no evidence for an atmospheric CO_2 enhancement of bauxitization at lower temperatures and precipitation (Bird et al. 1990) from these data, which cover a range of CO_2 orders of magnitude less than created naturally in soils by respiration (Brook et al. 1983).

Other factors in bauxitization not supported by this study are aluminous parent material, efficient leaching (Paton and Williams 1972), long duration

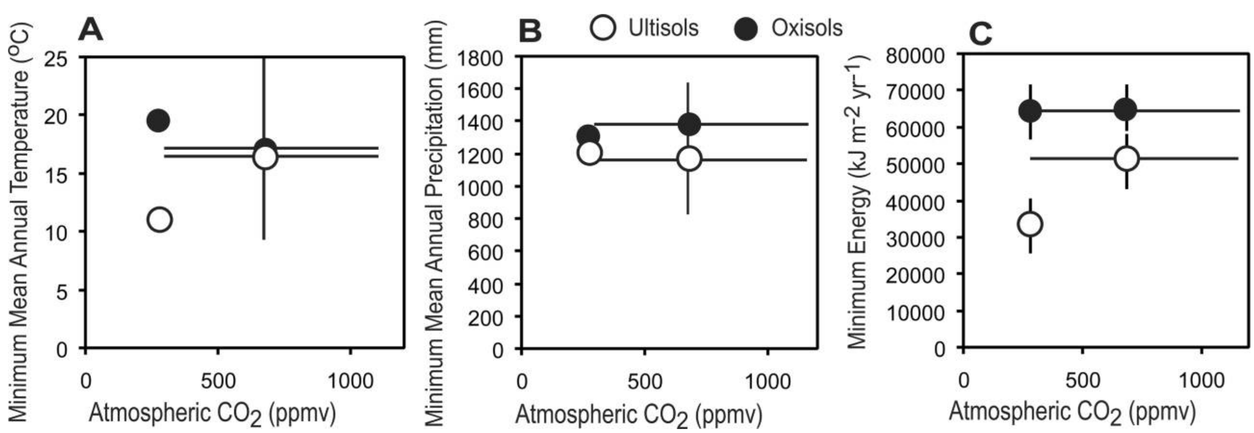

Figure 8. Paleoclimatic minima for Oxisols and Ultisols during times of Eocene elevated atmospheric CO_2, when Monaro Volcanics were active compared with their climatic distribution today (table 5). Errors are all 2 SE of transfer functions used.

of formation (Taylor et al. 1992), near-surface alteration of outcrops (Hunt et al. 1977), and continuous long-term alteration of surface outcrops (Bourman 1993). These factors are negated for the Monaro Volcanic paleosols by mafic parent materials (fig. 4), limited times for formation (fig. *6D*), and study entirely within the drill core (fig. 4). Nevertheless, these other factors remain theoretically feasible in geological circumstances other than thick sequences of comagmatic intrabasaltic paleosols.

ACKNOWLEDGMENTS

E. Reziak facilitated access to the Bega no. 7 core at Geoscience Australia, Canberra. B. Cramer offered useful discussion. Detailed reviews by N. Sheldon and C. Robert greatly improved the manuscript.

REFERENCES CITED

Alley, R.; Berntsen, T.; Bindoff, N. L.; Chen, Z.-L.; Chidthaisong, A.; Friedlingstein, P.; Gregory, J. M.; et al. 2007. Climate change 2007: the physical science basis. Geneva, Intergovernmental Panel on Climate Change, 1009 p.

Bird, M. I., and Chivas, A. R. 1989. Stable-isotope geochemistry of the Australian regolith. Geochim. Cosmochim. Acta 53:3239–3256.

Bird, M. I.; Chivas, A. R.; Fyfe, W. S.; and Longstaffe, F. J. 1990. Deep weathering at extratropical latitudes: a response to increased atmospheric CO_2. *In* Bouwman, A. F., ed. Soils and the greenhouse effect. Chichester, Wiley, p. 383–389.

Bishop, P. 1985. Southeast Australian late Mesozoic and Cainozoic denudation rates: a test for late Tertiary increases in denudation. Geology 13:479–482.

Bourman, R. P. 1993. Perennial problems in the study of laterite: a review. Aust. J. Earth Sci. 40:387–401.

Bowen, G. J., and Bowen, B. B. 2008. Mechanisms of PETM global change constrained by a new record from central Utah. Geology 36:379–382.

Bowen, G. J.; Koch, P. J.; Meng, J.; Ye, J.; and Ting, S. 2005. Age and correlation of fossiliferous late Palaeocene–early Eocene strata of the Erlian Basin, Inner Mongolia, China. Am. Mus. Novit. 3474:26.

Brook, G. A.; Folkoff, M. E.; and Box, E. O. 1983. A world model of soil carbon dioxide. Earth Surface Proc. Landforms 8:79–88.

Brown, M. C.; McQueen, K. G.; and Taylor, G. 1992. A core through the Monaro Basalt: Bega (BMR) no. 7. Aust. J. Earth Sci. 39:555–559.

———. 1994. Reply: a core through the Monaro Basalt: Bega (BMR) no. 7. Aust. J. Earth Sci. 41:71–72.

Carpenter, R. J.; Hill, R. S.; and Jordan, G. J. 1994. Cenozoic vegetation in Tasmania: macrofossil evidence. *In* Hill, R. S., ed. History of the Australian vegetation: Cretaceous to recent. New York, Cambridge University Press, p. 276–298.

Clement, B. M. 2004. Dependence of the duration of geomagnetic polarity reversals on site latitude. Nature 428:637–640.

Collinson, M. E. 1983. Fossil plants of the London Clay. London, Palaeontological Association, 21 p.

Dalrymple, G. B. 1979. Critical tables for conversion of K-Ar ages from old to new constants. Geology 7: 558–560.

Dickens, G. R.; O'Neil, J. R.; Rea, D. K.; and Owen, R. M. 1995. Dissociation of methane hydrate as a cause of the carbon isotope excursion at the end of the Paleocene. Palaeoceanography 10:965–971.

Food and Agriculture Organization. 1971. Soil map of the world. Vol. IV. South America. Paris, United Nations Educational, Cultural, and Scientific Organization, 193 p.

———. 1975*a*. Soil map of the world. Vol. II. North America. Paris, United Nations Educational, Cultural, and Scientific Organization, 210 p.

———. 1975*b*. Soil map of the world. Vol. III. Mexico and Central America. Paris, United Nations Educational, Cultural, and Scientific Organization, 96 p.

———. 1977*a*. Soil map of the world. Vol. VI. Africa. Paris, United Nations Educational, Cultural, and Scientific Organization, 299 p.

———. 1977*b*. Soil map of the world. Vol. VII. South Asia. Paris, United Nations Educational, Cultural, and Scientific Organization, 117 p.

———. 1978. Soil map of the world. Vol. IX. Australasia. Paris, United Nations Educational, Cultural, and Scientific Organization, 158 p.

———. 1979. Soil map of the world. Vol. IX. Southeast Asia. Paris, United Nations Educational, Cultural, and Scientific Organization, 140 p.

———. 1981. Soil map of the world. Vol. V. Europe. Paris, United Nations Educational, Cultural, and Scientific Organization, 199 p.

Greenwood, D. R.; Moss, P. T.; Rowett, A. I.; Vadala, A. T.; and Keefe, R. L. 2003. Plant communities and climate change in southeastern Australia during the early Paleogene. *In* Wing, S. L.; Gingerich, P. D.; Schmitz, B.; and Thomas, E., eds. Causes and consequences of globally warm climate in the early Paleogene. Geol. Soc. Am. Spec. Pap. 369:365–380.

Holdgate, G. R.; Wallace, M. W.; Gallagher, S. J.; Wagstaff, B. E.; and Moore, D. 2008. No mountains to snow on: major post-Eocene uplift of the East Victoria highlands: evidence from Cenozoic deposits. Aust. J. Earth Sci. 55:211–234.

Hunt, P. A.; Mitchell, P. B.; and Paton, T. R. 1977. "Laterite profiles" and "lateritic ironstones" on the Hawkesbury Sandstone, Australia. Geoderma 19: 105–121.

Idnurm, M. 1985. Late Mesozoic and Cenozoic palaeomagnetism of Australia. I. A redetermined apparent polar wander path. Geophys. J. R. Astron. Soc. 83: 399–418.

Ivany, L. C.; Lohmann, K. C.; Hasiuk, F.; Blake, D. B.; Glass, A.; Aronson, R. B.; and Moody, R. M. 2008. Eocene climate record of a high southern latitude continental shelf: Seymour Island, Antarctica. Geol. Soc. Am. Bull. 120:659–678.

Kent, D. V.; Cramer, B. S.; Lanci, L.; Wang, P.; Wright, J. D.; and van der Voo, R. 2003. A case for a comet impact trigger for the Paleocene/Eocene thermal maximum and carbon isotope excursion. Earth Planet. Sci. Lett. 211:13–26.

Koch, P. L.; Zachos, J. C.; and Gingerich, P. D. 1992. Correlation between isotope records in marine and continental carbon reservoirs near the Paleocene/ Eocene boundary. Nature 358:319–322.

Kraus, M. J., and Riggins, S. 2007. Transient drying during the Paleocene-Eocene thermal maximum (PETM): analysis of paleosols in the Bighorn Basin, Wyoming. Palaeogeogr. Palaeoclimatol. Palaeoecol. 245:444–461.

Kuagai, H.; Sweda, T.; Hayashi, K.; Kojima, S.; Basinger, J. F.; Shibuya, M.; and Fukuo, Y. 1995. Growth-ring analysis of early Tertiary conifer woods from the Canadian High Arctic and its paleoclimatic interpretation. Palaeogeogr. Palaeoclimatol. Palaeoecol. 116: 247–262.

Lourens, L. J.; Sluijs, A.; Kroon, D.; Zachos, J. C.; Thomas, E.; Roehl, U.; Bowles, J.; and Raffe, I. 2005. Astronomical pacing of late Paleocene to early Eocene global warming events. Nature 435:1083–1087.

Macphail, M. K.; Alley, N. F.; Truswell, E. M.; and Sluiter, I. R. K. 1994. Early Tertiary vegetation: evidence from spores and pollen. *In* Hill, R. S., ed. History of the Australian vegetation: Cretaceous to recent. New York, Cambridge University Press, p. 189–261.

Markewich, H. W.; Pavich, M. J.; Mausbach, M. J.; Hall, R. G.; Johnson, R. G.; and Hearn, P. D. 1987. Age relations between soils and geology in the Coastal Plain of Maryland and Virginia. U.S. Geol. Surv. Bull. 1589A, 34 p.

Mathews, R. H. 1908. Vocabulary of the Ngarrugu tribe, N.S.W. J. Proc. R. Soc. NSW 42:335–342.

Müller, M. J. 1982. Selected climatic data for a global set of standard stations for vegetation science. The Hague, Junk, 206 p.

Nesbitt, H. W., and Young, G. C. 1989. Formation and diagenesis of weathering profiles. J. Geol. 97:129–147.

Pancost, R. D.; Steart, D. S.; Handley, L.; Collinson, M. E.; Hooker, J. J.; Scott, A. C.; Grassineau, N. V.; and Glasspool, I. J. 2007. Increased terrestrial methane cycling at the Paleocene-Eocene thermal maximum. Nature 449:332–335.

Parrish, J. T. 1998. Interpreting pre-Quaternary climate from the geologic record. New York, Columbia University Press, 338 p.

Paton, T. R., and Williams, M. A. J. 1972. The concept of laterite. Ann. Assoc. Am. Geogr. 62:42–56.

Pearson, P. N., and Palmer, M. R. 2000. Atmospheric carbon dioxide concentrations over the past 60 million years. Nature 406:695–699.

Pratt, G. W.; Lewis, P. C.; Taylor, G.; Brown, M. C.; Roach, I. C.; and McQueen, K. G. 1993. The Monaro Volcanics of the Cooma district. Q. Notes Geol. Surv. NSW 92: 1–10.

Rainbird, R. H.; Nesbitt, H. W.; and Donaldson, J. A. 1991. Formation and diagenesis of sub-Huronian saprolite: comparison with a modern weathering profile. J. Geol. 98:801–822.

Rasmussen, C., and Tabor, N. J. 2007. Applying a quantitative energy model across a range of environmental gradients. Soil Sci. Soc. Am. J. 71:1719–1729.

Retallack, G. J. 2001*a*. A 300-million-year record of atmospheric carbon dioxide from fossil plant cuticles. Nature 411:287–290.

———. 2001*b*. Soils of the past. Oxford, Blackwell, 600 p.

———. 2005. Pedogenic carbonate proxies for amount and seasonality of precipitation in paleosols. Geology 33:333–336.

———. 2008*a*. Greenhouse crises of the geological past. Geol. Soc. Am. Bull., forthcoming.

———. 2008*b*. Mechanisms of PETM global change constrained by a new record from central Utah: comment. Geology, forthcoming.

Retallack, G. J.; Orr, W. N.; Prothero, D. R.; Duncan, R. A.; Kester, P. R.; and Ambers, C. P. 2004. Eocene-Oligocene extinction and paleoclimatic change near Eugene, Oregon. Geol. Soc. Am. Bull. 116:817–839.

Roach, I. C. 1994. Geochemistry, petrology and structural control of eruption centres in the Monaro Volcanic Province. *In* McQueen, K. G., ed. The Tertiary geology and geomorphology of the Monaro: the perspective in 1994. Cent. Aust. Regolith Stud. Occas. Publ. 2:37–43.

———. 1996. The formation of the Monaro Volcanic Province, southeastern NSW, Australia. *In* Stephenson, P. A., and Whitehead, P. W., eds. Chapman Conference abstracts: long lava flows. Contrib. Econ. Geol. Res. Unit, James Cook Univ. Townsville 56: 60–61.

———. 1999. The setting, structural control, geochemistry and mantle source of the Monaro Volcanic Province, southeastern New South Wales, Australia. PhD thesis, University of Canberra.

Robert, C., and Kennett, J. P. 1992. Paleocene and Eocene kaolinite distribution in the South Atlantic and Southern Ocean: Antarctic climatic and paleoceanographic implications. Mar. Geol. 103:99–101.

Ruffner, J. A. 1985. Climates of the states. Detroit, Gale, 1572 p.

Sharp, K. R. 1994. Discussion: a core through the Monaro Basalt: Bega (BMR) no. 7. Aust. J. Earth Sci. 41:69–70.

———. 2004. Cenozoic volcanism, tectonism and stream derangment in the Snowy Mountains and northern Monaro of New South Wales. Aust. J. Earth Sci. 51: 67–83.

Sheldon, N. D. 2003. Pedogenesis and geochemical alteration of the Picture Gorge Subgroup, Columbia River Basalt, Oregon. Geol. Soc. Am. Bull. 115:1377–1387.

———. 2006. Quaternary glacial-interglacial climate cycles in Hawaii. J. Geol. 114:367–376.

Sheldon, N. D; Retallack, G. J.; and Tanaka, S. 2002. Geochemical climofunctions from North American soils and application to paleosols across the Eocene-Oligocene boundary in Oregon. J. Geol. 110:687–696.

Sluijs, A.; Schouten, S.; Pagani, M.; Woltering, M.; Brinkhuis, H.; Sinninghe Damste, J. S.; Dickens, G. R.; et al. 2006. Subtropical Arctic Ocean temperatures during the Paleocene/Eocene thermal maximum. Nature 441:610–613.

Soil Survey Staff. 2000. Keys to soil taxonomy. Blacksburg, VA, Pocahontas, 600 p.

Stephens, J. C., and Hering, J. G. 2002. Comparative characterization of volcanic soils exposed to decade-long elevated CO_2 concentrations at Mammoth Mountain, California. Chem. Geol. 186:301–313.

Svensen, H.; Planke, S.; Malthe-Sørenssen, A.; Jamtveit, B.; Myklebust, R.; Eidem, T. R.; and Rey, S. S. 2004. Release of methane from a volcanic basin as a mechanism for initial Eocene global warming. Nature 429: 542–545.

Tabor, N. J., and Montañez, I. P. 2005. Oxygen and hydrogen isotope composition of Permian pedogenic phyllosilicates: development of modern surface domain arrays and implications for paleotemperature reconstructions. Palaeogeogr. Palaeoclimatol. Palaeoecol. 223:127–146.

Tabor, N. J., and Yapp, C. J. 2005. Coexisting goethite and gibbsite from a high-palaeolatitude (55°N) Late Paleocene laterite: concentration and $^{13}C/^{12}C$ ratios of occluded CO_2 and associated organic matter. Geochim. Cosmochim. Acta 69:5495–5510.

Taylor, G.; Eggleton, R. A.; Holzhauer, C. C.; Maconachie, C. A.; Gordon, M.; Brown, M. C.; and McQueen, K. G. 1992. Cool climate lateritic and bauxitic weathering. J. Geol. 100:669–677.

Taylor, G.; Taylor, G. R.; Bink, M.; Foudoulis, C.; Gordon, M.; Hedstrom, J.; Minello, J.; and Whippy, F. 1985. Prebasaltic topography of the northern Monaro and its implications. Aust. J. Earth Sci. 32:65–71.

Taylor, G.; Truswell, E. M.; McQueen, K. G.; and Brown, M. C. 1990. Early Tertiary palaeogeography, landform evolution and palaeoclimate of the southern Monaro, NSW, Australia. Palaeogeogr. Palaeoclimatol. Palaeoecol. 78:109–134.

Wellman, P., and McDougall, I. 1974. Potassium-argon ages on the Cainozoic rocks of New South Wales. Geol. Soc. Aust. J. 21:247–272.

Wing, S. L.; Harrington, G. J.; Smith, F. A.; Bloch, J. I.; Boyer, D. M.; and Freeman, K. M. 2005. Transient floral change and rapid global warming at the Paleocene-Eocene boundary. Science 310:993–996.

Young, R. W., and McDougall, I. 1985. The age, extent and geomorphological significance of the Sassafras Basalt, southeastern New South Wales. Aust. J. Earth Sci. 34: 323–331.

Zachos, J.; Pagani, M.; Sloan, L.; Thomas, E.; and Billups, K. 2001. Trends, rhythms, and aberrations in global climate 65 Ma to present. Science 292: 686–693.